Proceedings of the 11th Brazilian Congress of Thermal Sciences and Engineering -- ENCIT 2006
Braz. Soc. of Mechanical Sciences and Engineering -- ABCM, Curitiba, Brazil, Dec. 5=8, 2006

Paper CIT06-0553

THE EFFECT OF THERMAL RADIATION MODELS P-1 E DO ON THE CALCULATION OF TURBULENT REACTIVE FLOW MODELED WITH RSM OR RNG k-ε.

Fábio Alfaia da Cunha
Departamento de Engenharia Mecânica, Centro Tecnológico, Universidade Federal do Pará.
Rua Augusto Corrêa S/N, Guamá, Belém – PA – Brasil, CEP: 66075-110
alfai@ufpa.br

Pedro Andrey Cavalcante Sampaio
Departamento de Engenharia Mecânica, Centro Tecnológico, Universidade Federal do Pará.
Rua Augusto Corrêa S/N, Guamá, Belém – PA – Brasil, CEP: 66075-110
asampaio@ufpa.br

Manoel Fernandes Martins Nogueira
Departamento de Engenharia Mecânica, Centro Tecnológico, Universidade Federal do Pará.
Rua Augusto Corrêa S/N, Guamá, Belém – PA – Brasil, CEP: 66075-110
mfmn@ufpa.br

Daniel Onofre de Almeida Cruz
Departamento de Engenharia Mecânica, Centro Tecnológico, Universidade Federal do Pará.
Rua Augusto Corrêa S/N, Guamá, Belém – PA – Brasil, CEP: 66075-110
doac@ufpa.br

abstract. *EBMA group seeks to use the CFD code Fluent to design efficient cyclone furnaces to carry out combustion of sawdust and air. The group is looking for a combination of models to represent the radiation heat transfer and turbulence phenomena in such way that they require a minimum of computing time and yet have an acceptable agreement with experimental data. This work performed a calculation for a two phase (solid and gas phases) flow in cyclone combustor modeling the chemical reaction with a Presumed PDF/mixture fraction model and evaluating solutions for four different combinations of thermal radiation (P-1 and Discrete Ordinate – DO) with turbulent models. The four results were compared and the pair RSM-DO was chosen as the model that produced most reasonable results and to be used in further calculations. P1-RNG k-ε and P1-RSM pair generated temperature above the adiabatic flame temperature or lower than the inflow air temperature. DO-RSM pair and DO-RNG k-ε models generated reasonable values. The option for DO-RSM was due the fact that this turbulence model has proved to predict results closer the experimental ones in cylindrical flows, what is the case in this study.*

Key words: thermal radiation models, turbulence models, cyclone furnaces.

1. Introduction

Most of the furnaces, traditionally used in the Amazon region, are of large dimensions and low efficiency, hich means, a low daily burning capacity. That limitation can be eliminated by some project optimization or by the use of some other furnace type. The cyclone furnace, for example, is one of the devices that can used to burn solid particles in suspension. The cyclonic combustion represents an alternative for the conventional suspension combustion, it has the advantage to operate with various types of fuels like saw dust any many others agricultural disposals.

The correct prediction of the flow field is a very important parameter to be considered on the project of a cyclone furnace. Due to it's tri-dimensional nature, the cyclonic flow is very complex. The mathematical model used to describe such flow is also very complex, and a very accurate and stable turbulence model must be used combined with a robust numerical method, in order to obtain consistent results. The present work shows the results obtained after the numerical simulation of the cyclonic chamber of the UFPa Energy, Biomass and environment Group Laboratory.

A comparison of two turbulence models RNG-k-ε and RSM was performed. Not only the accuracy of the above cited modes is analyzed, but also their convergence capacity. Two radiation models are compared too, the P-1 model and the DO model. The FLUENT v 6.0 was used to carry out the calculations

2. The cyclone combustor

A cyclone combustor is a cylindrical chamber where air and solid particles follows a spiral flow paths due the tangential entrance of the inflow in the combustion chamber. This kind of entrance promotes high coefficients for heat

and mass transfer and also high volumetric reaction rates, with values in the range of 4 to 8 MW/m3 (Ushima, 1999). This kind of furnace, shown in the figure 1, is in its final stage of construction at the Mechanical Engineering Laboratory of the UFPA. It is 4.0 m tall with 0.84 m internal diameter and will be used to produce experimental results to validate the computational calculations

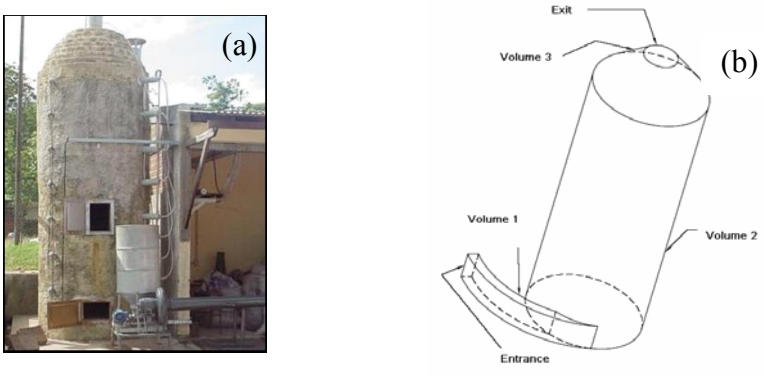

Figure 1. The cyclone furnace to obtain experimental data (a) and its geometry applied on calculations (b).

3. Geometry and mesh

All physical parameters needed were obtained from the cyclone furnace described in Figure 1(a) and the mesh needed for the Fluent to perform the calculation was built with the software Gambit. To simplify the mesh construction, the cyclone geometry was divided in three volumes: entrance, body and exit, as shown in Figure 1(b). Hexahedron cells were used to create the mesh. FLUENT (2003) directions to build a mesh for combustion case are: low EquiAngle Skew: <0.9, moderate aspect ratio (<10), smooth changing on cell volume (<30%), the cell boundary should be as orthogonal as possible. The mesh built has 0.66 as maximum EquiAngle skew and 7 as maximum Aspect ratio. The combustor mesh ended up with 105.000 cells.

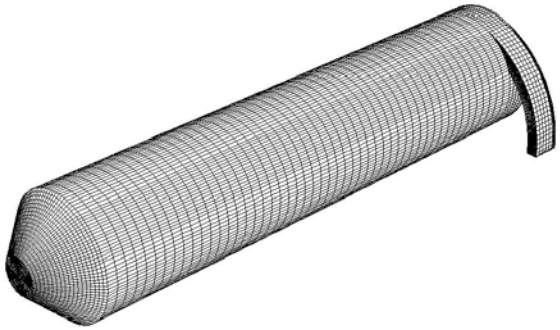

Figure 2. Combustor mesh.

4. Computational models

4.1 Turbulence models

Reynolds equations describe the turbulent flow. The most common way to close the Reynolds average Navier-Stokes equations is applying the Boussinesq hypothesis to related Reynolds stress to the mean velocity gradient, and this work will also do so. On the other hand, this work will not apply the regular k-ε model. Instead, one of its derivatives named RNG k-ε model (Orszag et al 1993) model was applied. In this last model the scales on the Navier-Stoke equation are deduced using the renormalization group theory. The authors choose such derivative because this one is based on constants and functions theoretically deduced in opposite the empirical ones used on the standard k-ε model.

In the Reynolds stress turbulence model, the closure of the equations involves the solution of a transport equation for each term of the Reynolds stress tensor. Besides that, an additional equation for a scalar equation (usually for ε) is needed. This means that seven equations must be solved simultaneously for the 3D case, as described in FLUENT (2003).

4.2. Model for combustion: Mixture fraction

The mixture fraction method is based on the solution for the transport equation for two conserved scalars named mixture fraction, ***f***, and its variance, $\overline{f'^2}$ in which a form for the PDF of the fluctuations in a conserved scalar is assumed (Sivathanu et al 1990). For a fuel/oxidizer system, the mixture fraction is defined as:

$$f = \frac{m_F}{m_F + m_{Ox}} \tag{1}$$

where *m* is mass, the subscript *Ox* denotes oxidizer and the subscript *F* means fuel.

4.3. Mathematical equations

Turbulent flows have its turbulent mass convection a few orders of magnitude bigger than the mass diffusion. In this case is reasonable to consider that the thermal diffusivity is equal to the molecular diffusion, Lewis number = 1 (Jones 1982), therefore all the conservation equations reduce to only one as a function of the mean mixture fraction, $\overline{f}$.

$$\frac{\partial}{\partial t}\left(\rho\bar{f}\right) + \nabla\left(\rho\vec{v}\bar{f}\right) = \nabla\left(\frac{\mu_t}{\sigma_t}\nabla\bar{f}\right) + S_m \tag{2}$$

where $\overline{v}$ is velocity, $\boldsymbol{\rho}$ is air density, μ_t is turbulent viscosity, and σ_t is turbulent Prandtl number. The source term Sm is due solely to mass transfer from solid particles into gas phase. The mixture fraction model also requires a solution for $\overline{f'^2}$ coming from the following conservative equation must be obtained.

$$\frac{\partial}{\partial t}\left(\rho\,\overline{f'^2}\right) + \nabla\left(\rho\vec{v}\,\overline{f'^2}\right) = \nabla\left(\frac{\mu_t}{\sigma_t}\nabla\,\overline{f'^2}\right) + C_g\mu_t\left(\nabla^2\bar{f}\right) - C_d\rho\frac{\varepsilon}{k}\overline{f'^2} \tag{3}$$

where $f' = f - \overline{f}$, temporal fluctuation of $\boldsymbol{f}.\sigma_t$, C_g and C_d are constants with values 0.85, 2.86 e 2.0, respectively defined at Fluent´s manual 2003. ε and k are the eddy dissipation rate and turbulence kinetic energy.
Scalar mean values due its variation during the turbulent fluctuations such as species concentration, density and temperature, they were evaluated with the help of the probability density function, PDF. This function describes the time fluctuation of ***f*** due the effects of chemical reaction and turbulent flow. In this work the PDF was modeled as a two-moment beta function, p(***f***), given for the following expression.

$$p(f) = \frac{f^{\alpha-1}(1-f)^{\beta-1}}{\int_0^1 f^{\alpha-1}(1-f)^{\beta-1}\,df} \tag{4}$$

where: $\alpha = \bar{f}\left[\bar{f}(1-\bar{f})/\overline{f'^2} - 1\right]$ and $\beta = (1-\bar{f})\left[\bar{f}(1-\bar{f})/f'^2 - 1\right]$

4.4. Model for the flow of the solid phase

Fluent uses a Lagrange description for the solid phase flow. The changing in properties during its moving through the gas phase is calculated through a set of ordinary differential equations representing the conservation equations of mass, momentum and energy. In this description, the initial solid phase properties and conditions are the input to start the calculation. The calculation results are the flow path, heat and mass transfer. The solid phase is dispersion in the gas phase was determined through the stochastic tracking model. The equations of heating, volatilization and carbon oxidation are integrated through the calculated particle path. The calculation starts with the particle drying, than the its volatilization and finally the particle oxidation, what now is coal, being oxidation the process which last long (Ragland et al. 1998). The model adopted to describe the volatilization is a first order reaction with a single kinetic rate.

$$-\frac{dm_p}{dt} = k\left[m_p - (1-f_{v,0})m_{p,0}\right] \tag{5}$$

where mp is the temporal particle mass (kg), $f_{v,0}$ is the initial volatiles mass fraction in the particle, $m_{p,0}$ is the initial mass particle (kg), k is the rate constant (s-1) following the Arrhenius definition for the rate constant: $k = A_1 e^{-(E/RT)}$. In this work A1 and E were defined as 7.0 E+7 s-1 and 1.2964 E+8 J/kgmol respectively (Ragland 1998).

The surface reaction is a sink for the oxidant species and a source of products species to the gas phase. In this work, a kinetic/diffusion-limited model was adopted and a heterogeneous reaction on the particle surface is represented for the equation (6).

$$\frac{dm_p}{dt} = -A_p P_{ox} \frac{D_0 \Re}{D_0 + \Re} \tag{6}$$

where A_P is the superficial area of a particle (πdp2), Pox is the oxidant partial pressure that surrounds a particle. The kinetic rate, $\Re = C_2 e^{-(E/RT_P)}$, incorporate the effects of chemical reaction on the internal surface of the char particle, residue of biomass volatilization and pore diffusion (C2 = 2E-3). The diffusion of the gaseous oxidant to the surface of the particle is given by,

$$D_0 = C_1 \left[\left(T_p - T_\infty \right) / 2 \right]^{0.75} / d_p \tag{7}$$

where T_P is the particle temperature, T_∞ is the local fluid temperature and C_1 is the mass diffusion limited rate constant with adopted value 5E-12.

4.5. Radiation models

The model P-1 is the simplest case of the P-N model which is based on the expansion of the radiation intensity on spherical harmonic orthogonal series FLUENT (2003). The model assumes that all the surfaces are diffuses, in other words, the reflection of the radiation that reaches some surface is isotropic. Besides that, the hypothesis of gray radiation is assumed. According to FLUENT (2003), for applications where the optical thickness is large the model P-1 works well. The optical thickness is defined as $(a+\sigma_s)$ L, where L is an appropriate characteristic length, which could be the furnace diameter for example. The equations that describe the model P-1 are show in FLUENT (2003).

The DO (Discrete ordinates) model solves de radiation heat transfer equation for a finite number of discrete solid angles; each one is related to the direction vector $\vec{S}$ defined at the global Cartesian system (x,y,z), the discrete mesh nodes are defined at the polar (θ, $0<\theta<\pi/2$) and the azimuthal (Φ, $0<\Phi<\pi/2$) directions. The model transforms the radiation heat transfer equation into a transport equation for the radiation intensities on the space coordinates (x,y,z), but the number of equations to be solved are less than the number of the vector $\vec{S}$ directions. Each octet of the angular space 4 π , at any space location is divided in $N_\phi \times N_\theta$ solid angles , each one having the width of ω_i which is called as control angle. The total number of transport equations to be solved is $8 N_\phi N_\theta$, in other words at least 8 equations are solved for each 3D space octet, the number o mesh nodes can be controlled by the Fluent v.6.0 user. The DO model assumes an anisotropic spread of the radiation and can be applied to any optical thickness which means that he model can be used for any degree of the medium opacity. The DO model is computationally, one of the most expensive

5. Simulated cases

The P-1 and DO models are extensively used to numerically simulate combustion. The P-1 model has some limitations, basically related to the optical thickness, but it is very popular in practical situations due to its relatively low computational cost (Ilbas, 2005). It is well known that the DO model shows a superior performance, since it can be used for any degree of the medium opacity. But as mentioned before, the DO model needs more computational resources and is more expensive than the P-1 model.

To compare the predictions of the above cited models four combustion cases were simulated, as show in table 1.

Table 1. Simulated cases identification.

Models→	Turbulence model		Radiation model	
Cases↓	RNG k-ε	RSM	P-1	DO
C1		x	x	
C2		x		x
C3	X		x	
C4	X			x

For all the simulated cases, the mixed fraction model /PDF for combustion were used. Based in some previous simulations, the angular mesh ($N_\phi \times N_\theta$) of 6x6 was adopted this means, that the radiation heat transfer equation was solved for 288 (8x6x6) directions for each control volume. For the solid phase, a single rate model, equation (3.38) was used to simulate the particles volatilization and for the fixed carbon-oxygen reaction, the model described by equation (3.56) was used. To describe the turbulent particle dispersion the DRW modes was adopted. The particles mass was distributed in 76800 trajectories. The mass, heat and momentum exchanges between the gas and the solid particles are also considered while the calculations were performed. The wood characteristics and thermal parameters are show in the tables 2 and 3 respectively.

Table 2. Fuel chemical composition.

Elemental analysis (%)		Immediate Analysis (%)	
C	52,70	Volatiles	31,50
H	6,01	Fixed Carbon	44,00
O	41,23	Ashes	1,99
N	-	Humidity	23,50
Cl	-	Inferior caloric power (MJ/kg)	19,77

Table 3. Properties and .some parameters used at the simulation.

Parameter	Value	Data source
Fuel Flow Rate	0,02 kg/s	-
Air Flow Rate	0,1475 kg/s	-
Density	650kg/m3	-
Cp	1760 J/kg-K	Van Wylen (1993)
Thermal Conductivity	0,173 w/m-K	Ragland (1998)
Gases absorption factor	Calculated using the wsggm model	
Volatilization model (single rate)	A=7e7s-1 E=1.2964e+008 J/kgmol	Ragland and Aerts, 1991
Combustion model (kinetics/diffusion-limited)	C1=5e-12 C2=0.002 E=79000000	Fluent standard values

6. Boundary conditions.

The no slip condition was used at the wall furnace. In the near wall region a Non Equilibrium Wall Function (Fluent 2003) was used to calculate the mean velocity and the turbulent kinetic energy. An air mass rate of 0.144 kg/s was used as an inlet condition. At the entrance the turbulent intensity and the length scale are respectively 10% and 0.056.

At the chamber exit, the pressure filed was calculated using equation (8). This equation assumes that the centrifugal forces created buy the swirl flow are balanced by the pressure gradient (FLUENT 2003).

$$\frac{\partial p}{\partial r} = \frac{\rho v_\theta^2}{r} \tag{8}$$

$$p(r=0) = p_0 \tag{9}$$

Where r is the radial coordinate v_θ is the tangential velocity and $\boldsymbol{p_0}$ is the pressure at the centerline which was considered as 101325Pa. In this case, a specific pressure condition is applied only at r =0. At the chamber exit the turbulent intensity was considered as 10% and the hydraulic diameter was equal 0.25.

The chamber walls are assumed as adiabatic with emissivity of 0.7. For the solid phase, the same parameters used in previous experiment performed at the UFPa Energy, Biomass and environment Group Laboratory cyclone furnace were used. It was represented by a ten diameter distribution between 20-40μm, each diameter is related to a mass fraction given by the Roisin-Rammler distribution function. The values of $\bar{d} = 161 \mu m$ and n= 3.67 were obtained after some adjustments based on experimental data. The initial positions of the particles were at the entrance region, the initial velocities were: ux=1.97m/s, uy=-6.71m/s e uz=0. The initial temperature was 308K. A 0.5 restitution coefficient was adopted (Fredriksson (1999)) after the collision of the particles with the wall. The carbon emissivity was adopted for the particles in suspension, which is 0.8 (Raglan and Aerts (1991))

7. Discussions and conclusion

The calculations took approximately 7 days to converge for each case. Table 4 shows the mean values of the molar fraction of the following substances CO, CO2, H2, N2, H2O and O2, calculated at chamber exit. No CO and H2 were found at the chamber exit for the C1 case. The molar values of CO2, N2, H2O and are of the same order of magnitude for each calculated case, in contrast, the values of CO and H2 are much smaller.

Table 4. Mean molar fraction at the furnace exit

	C1 (RSM+P1)	C2 (RSM+DO)	C3 (KE+P1)	C4 (KE+DO)
XCO	0,000000	0,000757	0,003306	0,005203
XCO2	0,095864	0,104196	0,086722	0,095808
XH2	0,000000	0,000139	0,001446	0,002085
XN2	0,741980	0,737190	0,743040	0,736600
XH2O	0,065617	0,071579	0,060190	0,067010
XO2	0,096611	0,086279	0,105411	0,093461

Obs: KE represents the RNG k-ε model

In order to help the analysis of the simulated cases, the distributions of CO, CO2, H2, N2, H2O and O2 at the central chamber plane are show below.

It can be seen that concentrations of CO and CO2 are higher at the chamber center, that is the region where the predictions between RNG/κ-ε and the RSN show the major difference. As can be seen in figure 3 the difference of the predictions for the mixture fraction field at the outlet region, given by the above cited modes, is remarkable. This fact is not really surprising since it is well known that the models which uses the turbulent viscosity concept are not adequate for swirl flows due to it's strong anisotropy (FREDRIKSSON, 1999).

In spite of the mean values of the molar fraction of CO2, N2, H2O and O2 are not so different at the outlet region for the four simulate cases, a closer inspection of the figures 5,6,7 and 9 reveals that the distribution inside of the furnace are greatly different for the C1,C2 and C3 cases. The C3 and C4 are the cases with closest results.

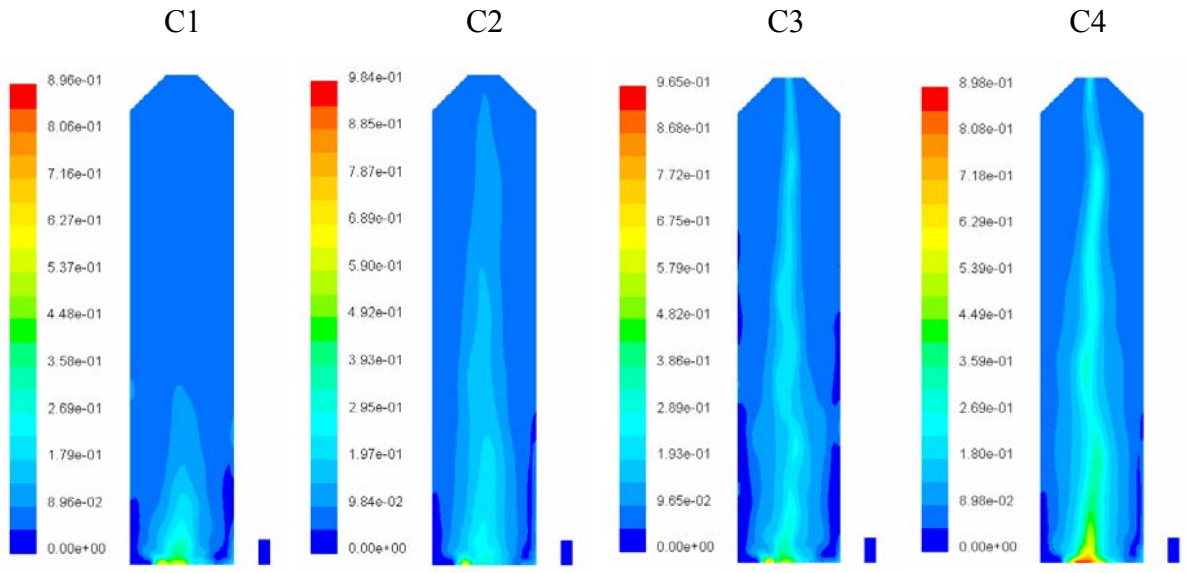

Figure 3. Mixture fraction distribution for C1, C2, C3 and C4 cases.

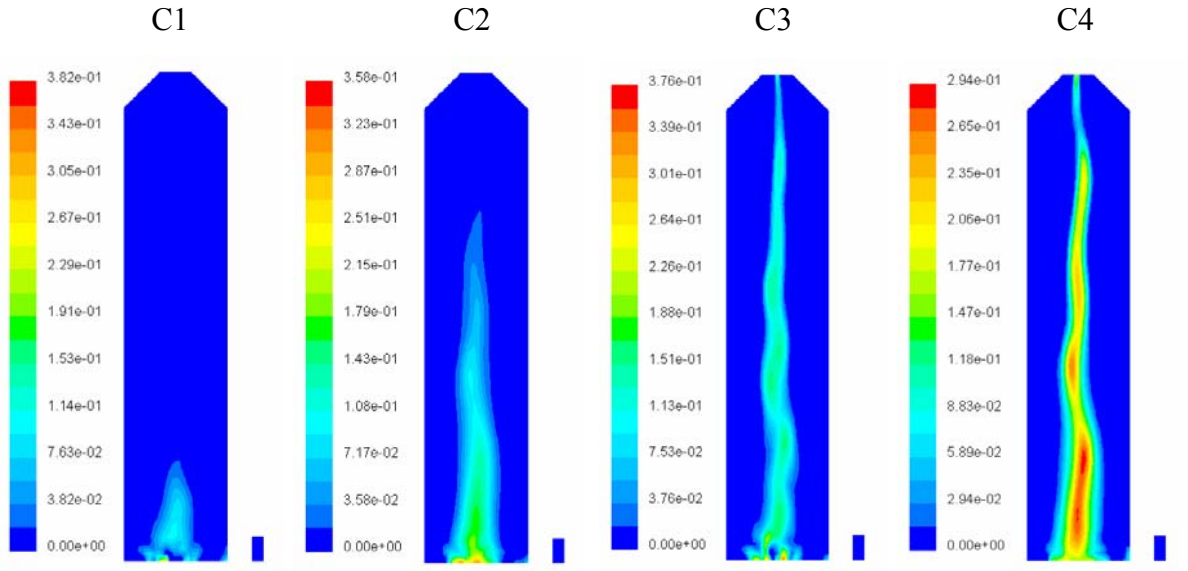

Figure 4. CO molar fraction distribution for C1, C2, C3 and C4 cases.

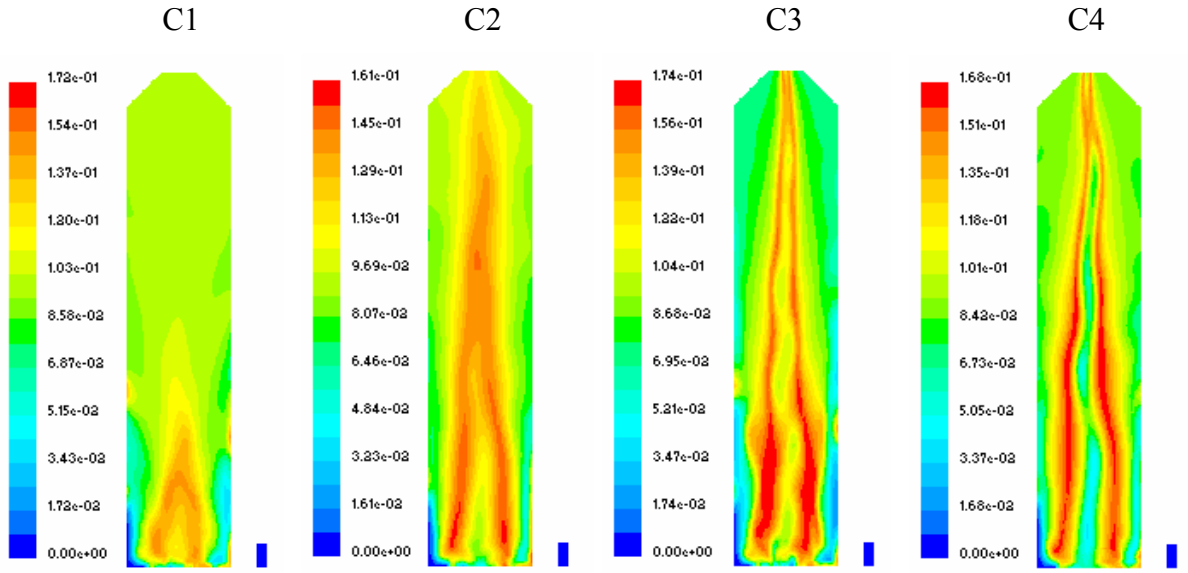

Figure 5. CO2 molar fraction distribution for C1, C2, C3 and C4 cases.

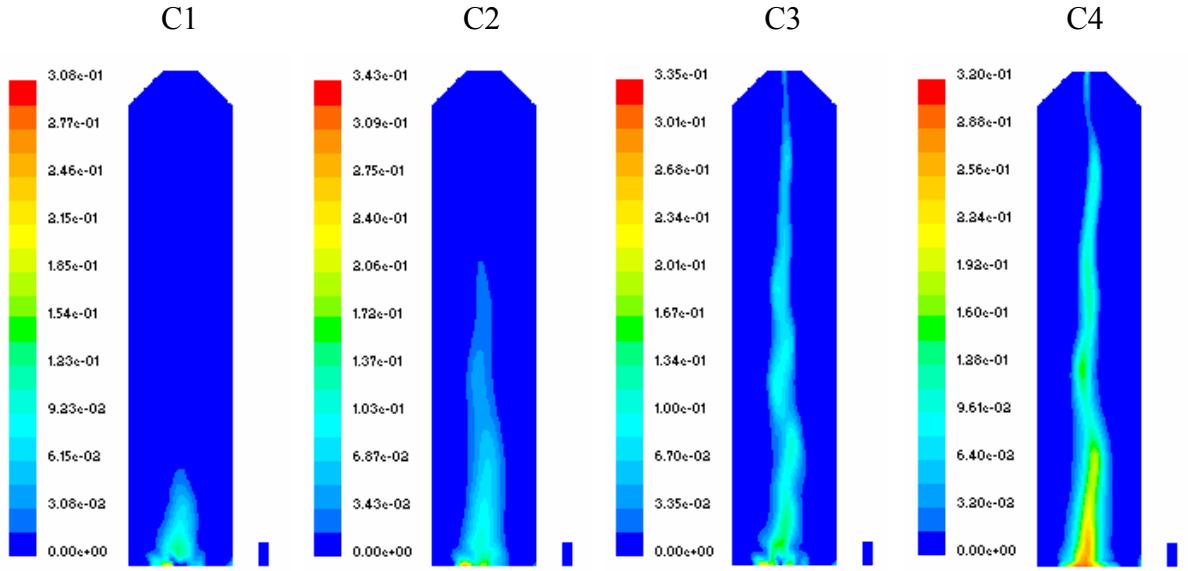

Figure 6. H2 molar fraction distribution for C1, C2, C3 and C4 cases.

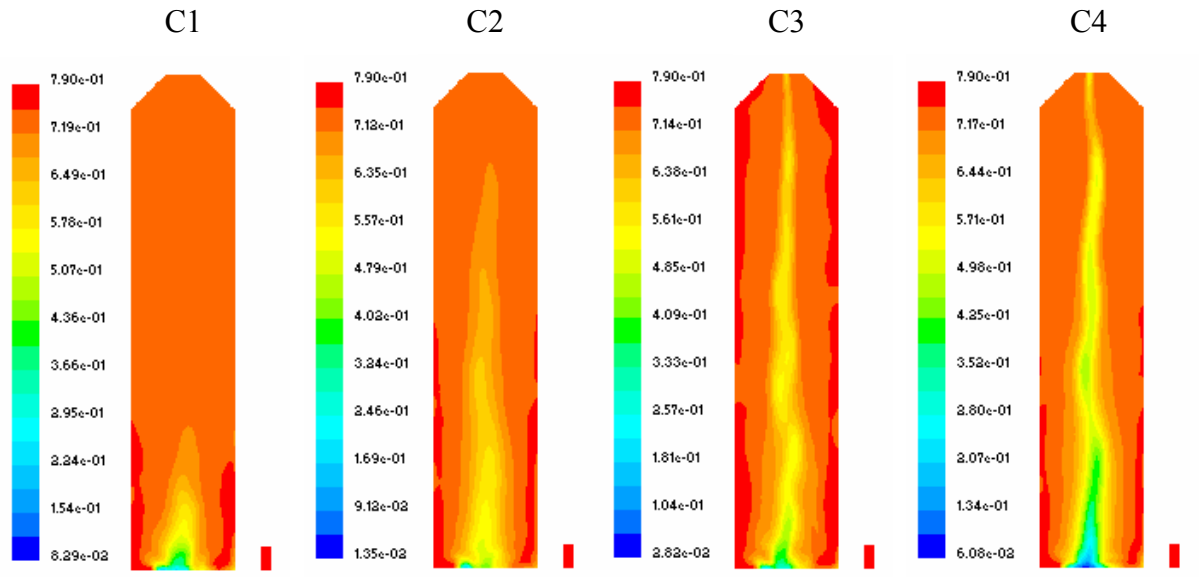

Figure 7. N2 molar fraction distribution for C1, C2, C3 and C4 cases.

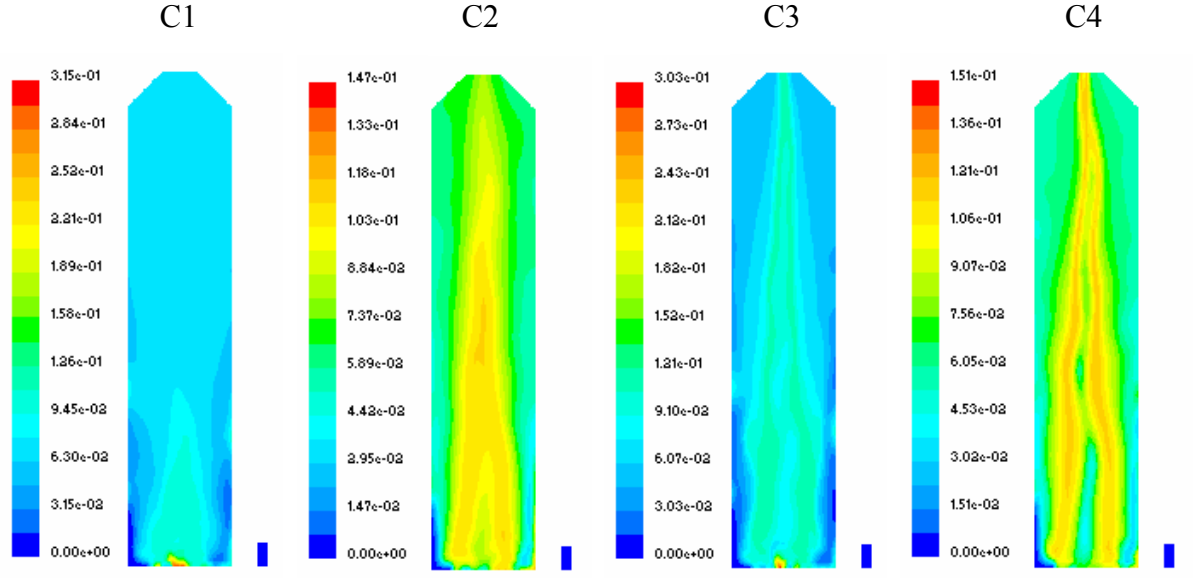

Figure 8. H2O molar fraction distribution for C1, C2, C3 and C4 cases.

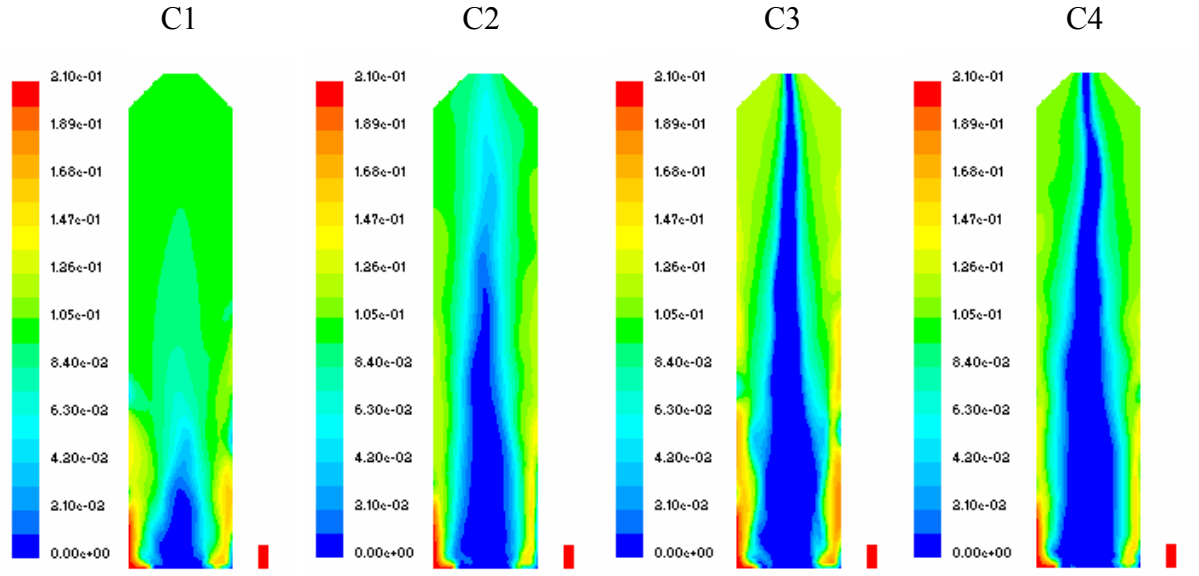

Figure 9. O2 molar fraction distribution for C1, C2, C3 and C4 cases.

The temperature fields are show in figure 10. For the C1 and C3 cases the maximum temperature limit was set at 1500K, this was done in order to allow the comparison of the temperatures by the color chard.

The maximum temperature recorded inside the furnace must be lower than the adiabatic flame temperature. The calculation of the flame temperature was performed using the prePDF and the obtained value was 2114K.The maximum calculated values of the temperature in the cases were the DO radiation model was used were 1990K and 1720K for the C2 and C4 case respectively. Those results are more precise than the results obtained with the P-1 radiation model. The P-1 model predicted some temperature peak higher than the adiabatic flame temperature (figure 10 and table 5), these results reveal some intrinsic inconsistency of the model. According to Sazhin et al (1995) the P-1 radiation model does not accurately predict the heat exchange process, in the presence of some concentrated heat sources. This deficiency can be the reason for the poor results obtained with the P-1 model. A second problem can be detected with the P-1 model, some predicted values of the temperature are lower than the values of the air temperature at the furnace entrance (see figure 10). Such behavior is not observed if the model DO is adopted. These results were only possible because a more tight angular $N_\phi \times N_\theta$ mesh was used, than the standard values of 2x2. The adopted values were 6x6. The increase of $N_\phi \times N_\theta$ nodes was jointed by a remarkable (7 times) increase in the computational time required for calculation, when compared with the standard pattern.

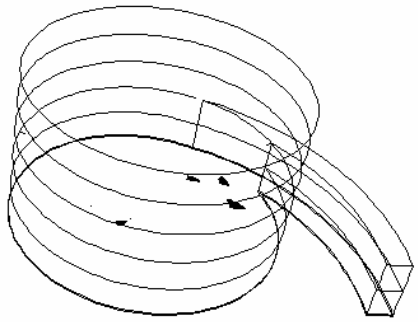

Figure 10: The black spots that appear near the entrance region, represents the places where temperatures above the adiabatic temperature were found for the C1 case.

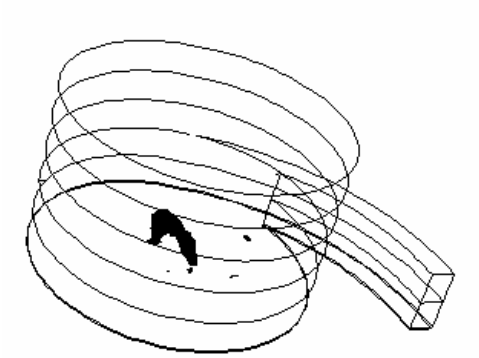

Figure 11. The black spots that appear near the entrance region, represents the places where temperatures above the adiabatic temperature were found for the C3 case.

Table 5. Significant temperatures found in the simulated cases.

Temperature	Case C1	Case C2	Case C3	Case C4
Maximum	2200K	1990K	2200K	1720K
Mean	1236K	1420K	1197K	1351K
Minimum	298K	308K	298K	308K

As can be seen in table 8 the C1 and C2 are the cases that show the higher mean temperatures. In the C1 case, as will be show in table 6, only 35% percent of the particles fixed carbon was released and as a result a smaller fuel quantity was used to increase the temperature of the furnace gases. The total release of the carbon that occurred in C2 case (table 9) is the reason for the higher mean temperature detected in this case, when compared with the other ones.

The permanence time, the volatile quantities and the fixed carbon liberated form the solid particles are show in table 6 .The solid phases calculation includes the particles tracking, volatilization and oxidation of the fixed carbon. Before comment the results, the term “particle destination” which appear in table 9 must be defined. In order to impose

a limit to the calculation of the path of a given particle a maximum length of 60m was imposed to the calculations. Depending on the particle trajectory it can go out of the furnace or stay inside of it after the 60m. The particles that reach the exit are called as "escape trough exit" the particles that stay in the furnace are referred as "incomplete". In this case the trajectories and all the calculation based on it are terminated. Because of that, in some cases, it will be reported that the conversion of the fixed carbon was not complete. In table 6 the percentage of conversion is calculated as:

$$\%Conv = 100(\text{Initial quantity} - \text{final quantity})/ \text{Initial quantity} \quad (3)$$

For all the simulated cases, the escape trough exit particles liberates all it's volatile substances and fixed carbon (%conv=100). For the incomplete trajectories particles it can be seen that only for the C2 and C4 cases (DO radiation model) the particles liberation of the fixed carbon was almost complete. For the C1 and C2 cases (P-1 radiation model), most of the fixed carbon was not liberated for the incomplete trajectories particles. If the maximum length adopted for the C1 and C2 cases was increased, maybe the particles fixed carbon would be totally released because that would have more time for them to perform some reactions, however that will dramatically increase the calculation time.

The mean time that the incomplete destination particle remain inside the furnace is larger if the Reynolds stress model is used (C1 and C2) when compared with the RNG κ-ε model (C3 and C4).

Table 6. Permanence time, volatile quantity, and fixed carbon of the solid particles.

	Particle destiny	Number of particles	Permanence time (s)				Volatile conversion (kg/s)			Fixed Carbon conversion (kg/s)		
			Mín	Máx	Mean	Standard Deviation	Initial quantity	Final quantity	%Conv	Initial quantity	Final quantity	%Conv
C1	Incomplete	24861	10,76	94,59	71,76	16,99	1,876E-03	0	100	2,621E-03	1,691E-03	35,49
	Escape trough exit	51939	1,439	56,63	7,989	5,937	2,900E-03	0	100	4,050E-03	0	100
	Particle destiny	Number of particles	Permanence time (s)				Volatile conversion (kg/s)			Fixed Carbon conversion (kg/s)		
			Mín	Máx	Mean	Standard Deviation	Initial quantity	Final quantity	%Conv	Initial quantity	Final quantity	%Conv
C2	Incomplete	12642	10,24	53	25,74	4,665	8,316E-04	0	100	1,162E-03	0	100
	Escape trough exit	64158	1,683	42,43	8,923	5,522	3,944E-03	0	100	5,510E-03	0	100
	Particle destiny	Number of particles	Permanence time (s)				Volatile conversion (kg/s)			Fixed Carbon conversion (kg/s)		
			Mín	Máx	Mean	Standard Deviation	Initial quantity	Final quantity	%Conv	Initial quantity	Final quantity	%Conv
C3	Incomplete	28382	9,23	87,67	49,62	20,29	2,193E-03	0	100	3,063E-03	1,487E-03	51,45
	Escape trough exit	48418	2,23	40,06	6,739	3,903	2,583E-03	0	100	3,609E-03	0	100
	Particle destiny	Number of particles	Permanence time (s)				Volatile conversion (kg/s)			Fixed Carbon conversion (kg/s)		
			Mín	Máx	Mean	Standard Deviation	Initial quantity	Final quantity	%Conv	Initial quantity	Final quantity	%Conv
C4	Incomplete	28470	9,25	94,14	43,23	19,82	2,219E-03	0	100	3,099E-03	1,139E-05	99,63
	Escape trough exit	48330	1,921	58,44	6,82	4,733	2,557E-03	0	100	3,572E-03	0	100

The differences of the flow field are obtained after the analysis of the swirl intensity, S, calculated for the four cases. The swirl intensity obtained for all the cases simulated here are show in figure 12. The results obtained with the RNG κ-ε model (C3 and C4) furnishes higher values of S for all the flow region, when compared with the Reynolds stress model (C1 and C2). Thus, as happened for the isotherm case, with the Reynolds stress model, S goes down at the entrance and at the exit of the furnace. For the first part of the furnace the predictions of S are different for all the simulated cases. The predictions of S are almost the same from Z=1m for C1 and C2. For the C3 and C4 the predictions are closer from Z=3m. For the cases the uses the same radiation model the observed differences are obviously due to the differences model. The cases which the RNG κ-ε turbulence model is used are more susceptible to the change of the radiation model than the cases where the Reynolds stress model is adopted. In all the case the differences of the predictions are smaller at the furnace exit.

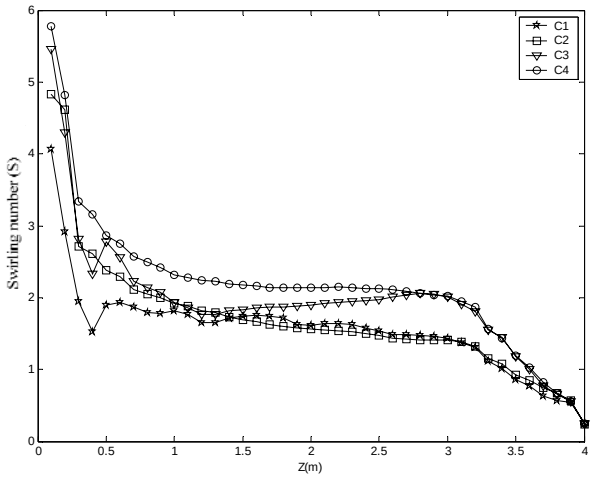

Figure 12. Swirl intensities for C1, C2, C3 and C4 cases.

.

After compare the performance of the models some conclusion can be obtained:

1) The temperature field obtained with the P-1 model is not realistic, since some calculated temperatures are higher than the flame temperature.
2) The differences of the results obtained with the radiation models are very high, almost 100%, because of that, the replacement of one model by the other must be done with care.
3) The differences of the predictions of the two turbulence modes were also very high. The molar fraction of CO and H2 predicted in the cases were the RNG κ-ε model was used are much higher than the results obtained with the Reynolds Stress model.

Based on the above results it can be concluded that the combination of the P-1 and the RNG κ-ε models is not suitable for the calculation of the combustion.

8. References

Berkstresser, B., Walz, A., Michael, V. and Timothy, G., 2000, .Combustion Improvements While Controlling Emissions., Proceedings of 2000 International Joint Power Generation Conference Miami Beach, Florida.

Bockelie, M. J., Eddings, E. G., Adams, B. R., Valentine, J. R., Cremer, M. A., Smith, P. J., Davis, K. A. and Heap, M. P., 1998, .Computational Simulations of Industrial Furnaces. International Symposium on Computational Technologies For Fluid/Thermal/Chemical Systems with Industrial Applications., San Diego, California, USA.

Eaton, A.M., Smoot, L.D., Hill, S.C. and Eatough, C.N., 1999.Components, formulations, solutions, evaluation, and application of comprehensive combustion models., Progress in Energy and Combustion Science., vol. 25, pp. 387. 436.

FLUENT Inc., 2003, .FLUENT 6.1, User's Guide Volume., vol. 1-4, Lebanon, USA.

Fredriksson, Chistian, 1999, .Exploratory Experimental and Theoretical Studies of Cyclone Gasification of Wood Powder., Doctoral Thesis, Divison of Energy Engineering, Department of Mechanical Engineering, Lulea University of Technology.

Ilbas, M. The Effect of Thermal Radiation and Radiation Models on Hydrogen-Hydrocarbon Combustion Modeling, International ournal of Hydrogen Energy, v. 30, p. 1113-1126, 2005.

Jones, W. P. and Whitelaw, J. H., Calculation Methods for Reacting Turbulent Flows, A Review. Combust. Flame, v.48, p. 1-26, 1982.

Kops, S. M. B. and Malter, P. C., 2004, .Simulation and Modeling of Wood Dust Combustion in Cyclone Burners., Final Technical Report Prepared for U. S. Department of Energy.

MALISKA, C. R., Transferência de Calor e Mecânica dos Fluidos Computacional. 2 ed. Rio de Janeiro: LTC, 2004.

Ragland, K. W., Aerts, D. J. and Baker, A. J., 1991, .Properties of Wood for Combustion Analysis., Bioresource Technology, vol. 37, pp. 161.168.

Ragland, K. W., and Borman, G. L., 1998, .Combustion Engineering., McGraw-Hill, USA.

Sazhin, S. S.; Sazhina, E. M.; Faltsi-Saravelou, O.; Wild, P. The P-1 Model for Thermal Radiation Transfer: Advantages and Limitations. Fuel, v. 75, p. 289-294, 1996.

Sivathanu, Y. R.; Faeth, G. M.. Generalized State Relationships for Scalar Properties in Nom-Premixed Hydrocarbon/Air Flames. Combust. Flame, v. 82, p. 211-230, 1990.

Syred, N. And Beér, J. M., 1974, .Combustion in swirling flows: A review., Combustion and Flame, Vol. 23, pp. 143-201.

Turns, S. R., 2004, .An Introduction to Combustion., McGraw-Hill, USA..

Ushima, A. H., 2000, .Curso de Combustão Industrial., Brasil.
Van Wylen, G. J. & Sonntag, R. E., 1976,.Fundamentos da Termodinâmica Clássica.; Edgard Blucher.